ISSN : 0917-415X DOI:10.3759/tropics.SIMM01

TROPICS Vol. 35 (1) ■ - ■ Issued June 1, 2026

ORIGINAL ARTICLE

Establishment of site- and species-specific allometric models of the dominant mangrove species and estimation of mangrove biomass in Letkhokkon Area, Myanmar

Kyaw Myo Lwin[1,2,*], Cao Thi Thu Hien[1] and Nyein Chan[3]

[1] Faculty of Silviculture, Vietnam National University of Forestry, Street 21, Xuan Mai Town, Chuong My District, Hanoi 100000, Vietnam
[2] Faculty of Forest and Environment, Eberswalde University for Sustainable Development, Schicklerstraße 5, 16225 Eberswalde, Germany
[3] Kyoto University of Advanced Science, Kameoka, Kyoto 621−8555 Japan
* Corresponding author: kyawmyolwin1995kml@gmail.com

Received: September 25, 2024 Accepted: June 24, 2025 J-STAGE Advance published date: December 23, 2025

ABSTRACT This study was conducted in the Letkhokkon delta mangrove, Myanmar to establish species-specific allometric models for accurate aboveground biomass estimation, contributing to improved mangrove ecosystem management. We found three mangrove species (*Avicennia officinalis*, *Sonneratia apetala* and *Sonneratia caseolaris*), and the first two species (*A. officinalis* and *S. apetala*) were dominant. Results highlighted the distinctive stand structure, species composition, and the low Shannon diversity ($H' = 0.734$). Using the tree measurable parameters such as diameter at breast height (*DBH*), height (*H*) and wood density (ρ), we established several allometric models of aboveground biomass ($W = ax^b$) for two dominant species. We selected the best-fit allometric models by model selection parameters. Also, we compared these best-fit models with the previously reported allometric models. Our study found that volumetric parameter (DBH^2H) and ρDBH^2H gave the best results with relatively higher accuracy than the other explanatory parameters. The study confirmed the importance of ρ in building of site-specific allometric model and also validated the superiority of species-specific models over generalized equations to estimate the biomass accurately. Besides, comparisons with other allometric models for mangroves in Americas, Asia, China and Myanmar emphasized the significance of tailored approaches, considering the influence of ρ on accurate biomass estimation. Wood density showed less significance in species-specific level though ρ was an important variable for generalized models. Applying ANOVA results for model comparison, the current models did not significantly differ from the previous ones. Furthermore, the mean biomass differences of current study were the least variations from the observed data among other models. It pointed out site- and species-specific models reduce the uncertainties of biomass and carbon stock estimations in comparison with the generalized models. Using the best-fit models, aboveground biomass of *Avicennia officinalis* stand were estimated as 13 Mg ha^{-1} and *Sonneratia apetala* stand, 14 Mg ha^{-1} of carbon. In conclusion, our study established the site- and species-specific equations for estimating mangrove biomass in Myanmar, with implications for Greenhouse gas (GHG) accounting and emission reduction.

Key words: mangrove biomass, species-specific allometric models, *Avicennia officinalis*, *Sonneratia apetala*, Myanmar

INTRODUCTION

Mangrove ecosystems are invaluable for their numerous ecosystem services, including shoreline protection, carbon sequestration, and providing habitats for various wildlife (Salem and Mercer, 2012). Yet, a critical challenge in understanding and quantifying the ecological value of these unique coastal forests lies in accurately estimating their biomass (Selvaraj and Gallego Pérez, 2023). Mangrove trees' distinctive form and the challenges of conducting field surveys in their waterlogged environments have hindered comprehensive exploration of their biomass, hampering our ability to assess their contribution to global carbon budgets and the services they provide (Salem and Mercer, 2012; Wang et al., 2019).

Mangroves are composed of diverse tree species, each with distinct morphological and ecological characteristics (Wang et al., 2019). Consequently, it is crucial to establish



Copyright © 2025 The Japan Society of Tropical Ecology. This is an open access article distributed under the terms of Creative Commons Attribution License (CC BY), which permits unrestricted use, distribution, and reproduction in any medium, provided the original source is properly credited. DOI:10.3759/tropics.SIMM01

species-specific allometric models to estimate their biomass accurately (Salem and Mercer, 2012; Selvaraj and Gallego Pérez, 2023; Wang et al., 2019). These models typically rely on measurable parameters such as Diameter at Breast Height (*DBH*), tree height (*H*), and wood density (ρ) (Komiyama et al., 2002; Komiyama et al., 2005). In the field, *DBH* and *H* can be easily measured and also the importance of ρ should be considered for building of the allometric models because the combination of *DBH*, *H* and ρ can enhance the accuracy of the model (Kusmana et al., 2018).

While allometric equations are potent tools for biomass estimation, establishing them often necessitates destructive, laborious and costly methods (Komiyama et al., 2005). The utilization of general or pre-established allometric models is a common practice due to the laborious nature of the destructive approach (Schindler et al., 2023). However, these generalized models may not accurately capture the variability in biomass across different species of mangroves, emphasizing the need for species-specific equations tailored to the local context (Kirue et al., 2006; Schindler et al., 2023).

In recent decades, several studies have focused on developing allometric equations for mangroves at global scale (Chave et al., 2005; Komiyama et al., 2008, 2005, 2002, 2000; Suzuki and Tagawa, 1983; Tamai et al., 1986). They established the equations using generally *DBH*, *H* and ρ as explanatory variables to estimate the mangrove biomass. Thant et al. (2012) conducted the first study for carbon sequestration potential of mangrove in Ayeyarwady delta, Myanmar, by establishing general allometric equations for six mangrove species to estimate aboveground and belowground biomass and comparing the sequestration rate of mangrove plantations and natural mangrove forests. Nonetheless, given the remarkable diversity of mangrove species in Myanmar, site- and species-specific equations are still required to estimate biomass accurately. Also in Myanmar, where mangrove ecosystems abound, the availability of reliable biomass data remains limited and continues to be an essential requirement for comprehensive understanding and management of these ecosystems.

To fill the research gap, we conducted this study in the Letkhokkon delta mangrove area in Kungyangon Township, Yangon, Myanmar including analyzing the stand structure and species composition in Letkhokkon's natural mangrove forests, and developing the species-specific allometric models for the two dominant mangrove species. The insights gained from this research will contribute significantly to the accurate estimation of mangrove aboveground biomass for this mangrove area in Myanmar, contributing to the fundamental information in this field and aiding in the effective management of these vital coastal ecosystems.

MATERIAL AND METHODS

Study site

Myanmar boasts a sprawling coastline extending from the Bay of Bengal in the west to the Andaman Sea in the south. Mangrove forests are found in three primary regions along this coastline: Rakhine State, Ayeyarwady Region, and Tanintharyi Division. Myanmar ranks third in Southeast Asia (Giesen et al., 2007) and seventh globally (Bunting et al., 2018) for its substantial mangrove coverage, encompassing 5,011 square kilometers, which represents 3.6% of the world's total mangrove areas (Bunting et al., 2018).

Letkhokkon area is not only been a prominent beach for several decades but also represents the first site in Myanmar where a natural beach was transformed into a thriving mangrove forest after 2004 tsunami (Dec 26, 2004), leading to the deposition of significant sediment loads on the beach. Additionally, its proximity to the estuaries of the Ayeyarwady River and Yangon River contributes to an annual deposition of sediments, fostering the development of various mangrove species. Furthermore, mangrove plantations have been established using the Regeneration Improvement Felling (RIF) technique in the rest of the mudflat areas by Worldview International Foundation (WIF) since February 2019. The RIF technique, a labor-intensive but highly effective method, involves site preparation by eliminating unwanted weeds for seedling spacing, enhancing sunlight exposure for seedlings by trimming unnatural branches, and promoting natural regeneration by selectively felling unhealthy trees.

Our study was performed in the Kanyashe Protected Public Forest, covering an area of 487 acres, situated in the Letkhokkon area (coordinates 16°20.093′−16°21.164′N and 96°9.488′−96°12.765′E) within the Kungyangon Township, Yangon region, Myanmar (Fig. 1). Initially, this area was a beach facing the Gulf of Mottama; however, after the 2004 Tsunami, sediments were deposited, transforming the beach into mudflats. The annual sediment deposits near the river estuaries provided favorable conditions for the growth of mangrove species. In 2015, the Forest Department (FD) officially designated 487 acres as the Kanyashe Protected Public Forest, and in 2019, an additional 1,507 acres were included. This site now stands as Myanmar's pioneering example of a natural mangrove forest rejuvenating a former beach habitat.

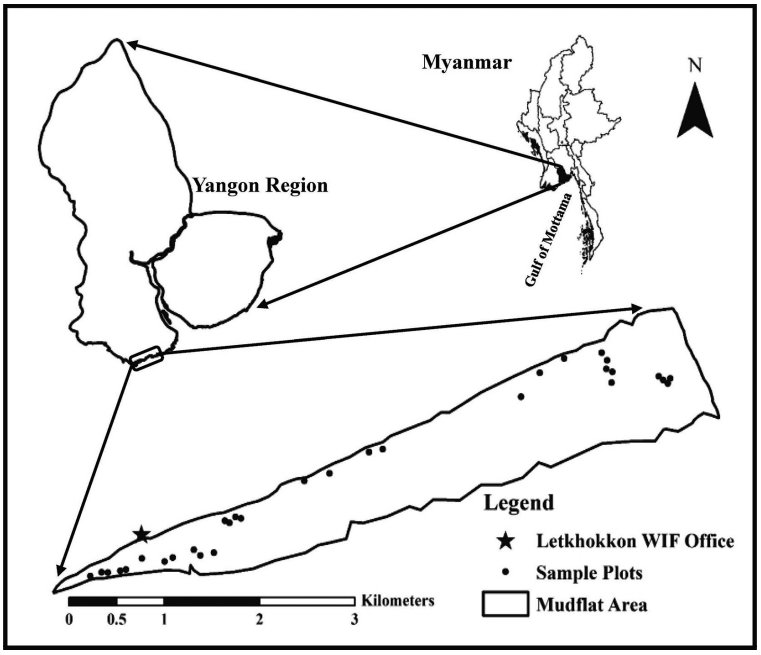


Fig. 1. Map showing the study site and sample plots conducted in mudflat area.

The regional climate in this area is characterized by monsoon seasons, with maximum temperatures peaking at around 40˚C in April and minimum temperatures dropping to approximately 19˚C in December over the past decade, as reported by the Kungyangon Agricultural Department. The study site receives an average annual rainfall of 2,777 millimeters and is situated at an above-sea-level elevation of roughly 3 meters. The prevailing soil types in this region include silt, loamy sand, and loamy clay. The pH levels of the brackish water in this area ranges typically from 7.7 to 8, with higher values occurring during the hot season. Salinity levels vary between 19 and 26 parts per thousand (ppt), with lower levels during the rainy season and higher levels during the hot season due to evaporation (Khin and Soe, 2019).

Methods

Sample plot establishment and tree measurement

Prior to the field trip, sample points were randomly set up on Google Earth Pro. Thirty-one 10 m × 10 m sample plots were then established on existing natural mangrove areas using GPS devices (GPSMAP 78 s, GARMIN). Some prior plots were not suitable to collect data in the field because of practical inconveniences related to topographic conditions were and decided to move a little from the original points. The selected plots were spaced at least 60 m apart. In each plot, all trees with a diameter at breast height (*DBH*) of 5 cm or greater were measured at 130 cm from the ground for both *DBH* and total tree height (*H*).

Biomass measurement and oven drying

Thirty sample trees of *Avicennia officinalis* (Ao) and *Sonneratia apetala* (Sa) were harvested to establish allometric models for estimating biomass. The *A. officinalis* had a *DBH* range of 5.0 cm to 13.0 cm and a *H* range of 5.6 m to 8.2 m. The *S. apetala* had a *DBH* range of 5.1 cm to 20.0 cm and a *H* range of 4.6 m to 13.6 m.

The selected trees were cut down at ground level, and their leaves, twigs, branches, and trunks were separated. The trunks were then divided into logs at ground level (D_0), at a height of 0.3 meters ($D_{0.3}$), and at intervals of 1 meter ($D_{1.3}$, $D_{2.3}$, $D_{3.3}$, and so on). These logs were weighed to obtain their fresh weight. Similarly, the leaves and the branches were weighed to determine the fresh biomass of each component of individual tree. Thirty representative parts from each tree (100 grams of leaves, 300 grams of branches, and 1−3 cm thick discs from every 1-meter logs for the trunk) were taken as samples and weighed in the field using an electronic balance to obtain their fresh weights. Subsequently, these parts were transported to the Forest Research Institute (FRI), Yezin, to obtain the dry/fresh weight ratio for each component. The woody biomass was dried in oven at 105˚C until a constant weight was achieved, while the non-woody biomass was dried at 65˚C (Phan et al., 2019). The dry weights of each component for the individual sample tree were calculated based on the dry/

fresh weight ratio obtained from the samples.

In addition, approximately 10 cm thick trunk discs (2–5 samples per tree) were taken to determine the wood density (ρ) of the trees. The green volume (cm^3) of each sample was measured on-site using the water displacement method. After drying the samples, their dry weights (g) were quantified using an electronic balance (BL-220 H, Shimadzu) with a readability of 0.001 g. The wood density of each sample tree was then calculated by dividing the dry weight (g) by the green volume (cm^3) of each trunk disc sample.

Data analysis

Stand structure, species composition and diversity

To assess the mangrove stand, we conducted an analysis of its structural characteristics, including the mean values of *DBH*, *H*, basal area, and stand density. Additionally, we employed three measures to investigate species composition: relative density (expressed as stems per hectare), relative dominance by basal area (measured in square meters per hectare), and relative frequency. To determine the significance of each species within the stand, we calculated their Importance Value (IV) using the method outlined by Cintron and Novelli (1984) as follow:

$$\text{Relative Density} = \frac{\text{Number of individuals of a species}}{\text{Total number of individuals}} \times 100$$

$$\text{Relative Dominance} = \frac{\text{Total basal area of a species}}{\text{Basal area of all species}} \times 100$$

$$\text{Relative Frequency} = \frac{\text{Frequency of a species}}{\text{Sum-frequency of all species}} \times 100$$

$$\text{Importance Value left(IVright)} = \text{Relative Density} + \text{Relative Dominance} + \text{Relative Frequency}$$

The diversity of mangrove species in the study was assessed using the Shannon diversity index (Magurran, 2003), which is calculated using the equation provided below:

$$H' = -\sum p_i \ln p_i$$

where H' represents the Shannon diversity index, and p_i represents the proportion of each species relative to the total number of species.

Besides, we calculated the dry/fresh weight ratio of each component of individual samples, as well as ρ.

Model establishment, and model comparisons

Utilizing the data obtained through destructive sampling, we established allometric equations of each dominant species and mixed ones in SPSS (Version 23) using the Curve Estimation procedure with a power function form $y = ax^b$ (Chan et al., 2013; Huy et al., 2016; Kusmana et al., 2018). In this function, y represents biomass (kg) and x represents *DBH* (cm), *DBH H* (cm m), DBH^2 *H* (cm^2 m), ρ *DBH* ($g\,cm^{-3}$ cm), ρ *DBH H* ($g\,cm^{-3}$ cm m) or ρ DBH^2 *H* ($g\,cm^{-3}\,cm^2$ m). Although the data were not manually transformed, SPSS internally applies a logarithmic transformation and fits the model using Ordinary Least Squares (OLS) regression on the transformed variables ($\ln y = \ln a + b \ln x$). The model coefficients (a and b) are then back-transformed to their original scale. We established the species-specific allometric models for each biomass component and total aboveground biomass, although only the models for total aboveground biomass were developed for mixed species.

To determine the best-fit models, we considered larger values of R^2 and smaller values of Standard Error of the Estimate, Residual Sum of Square (RSS) and Mean Square Error (MSE) in that order. We also tested whether the species-specific model outperforms the mixed one does. Furthermore, we compared our best-fit equation for aboveground biomass with those reported in previous studies conducted in Americas, Asia, China, and Myanmar (Chave et al., 2005; Komiyama et al., 2005; Ren et al., 2010; Thant et al., 2012). Using least significant difference (LSD) test of one-way ANOVA (Chan et al., 2013), a comparison of mean biomass differences between the present study and previously conducted models was made at 95 % confidence level. The lower/upper bound and significance level of each model were also tested to know the estimation accuracy over the observed field data.

Additionally, using the best-fit allometric models, we estimated the total aboveground biomass of both Ao and Sa species stands at plot level. For conversion from biomass to carbon, the default value 0.5 was used as a carbon fraction because the carbon concentration of wood is usually a little less than 50 % and local or species-specific values were not available (Kauffman and Donato, 2012).

For all analyses, we utilized IBM SPSS Statistics 23 for Windows, Microsoft Excel 2013, and Stata software.

RESULTS AND DISCUSSION

Stand structure, and species composition and diversity

In the study area, identified three prominent mangrove species: *Avicennia officinalis* (referred to as Ao), *Sonneratia apetala* (referred to as Sa), and *S. caseolaris* (referred to as Sc). The mean diameter and height with standard deviation

of the three species were respectively 7.11 ± 1.84 cm and 5.57 ± 0.91 m for Ao, 9.02 ± 3.69 cm and 7.70 ± 2.50 m for Sa and 10.64 ± 3.79 cm and 6.02 ± 1.09 m for Sc (Table 1). The cumulative basal area of Ao was 8.69 ± 3.88 m^2 ha^{-1}, 9.88 ± 9.23 m^2 ha^{-1} for Sa, and 8.24 ± 6.13 m^2 ha^{-1} for Sc, respectively. The stand density of these natural forests was quantified as 2,052 trees per hectare for Ao, 1,325 trees per hectare for Sa, and 825 trees per hectare for Sc, respectively. Furthermore, Sc occupied a relatively minor portion (5.0 %) in the western region, while Sa covered a comparatively larger area (24.0 %) in the central zone, and the largest expanse was dominated by Ao (71.1 %) in the eastern part of the study area. These findings highlight that Ao played a predominant role in the overall composition of the study site, with an importance value (IV) of 186.9 %, followed by Sa with an IV of 88.47 %, and Sc as the least dominant species with an IV of 24.6 %. As described in the Table 1, the diversity index of Ao was 0.243, followed by Sa (0.342) and Sc (0.149). The overall species diversity within the study site was notably low, as indicated by a Shannon index (H') of 0.734.

Dry/fresh weight ratio and wood density (ρ) of dominant species

The dry/fresh weight ratios of trunk and branch for both species were nearly the same (Table 2). The ratios of trunk are 0.483 and 0.433 for Ao and Sa, respectively. Also, Ao gave the dry/fresh weight ratio of branch 0.474, and Sa showed 0.429. However, the dry/fresh weight ratio of Ao leaf 0.358 was a little higher than 0.257 of Sa leaf. The leaf dry/fresh weight ratio in Sundarban (Chanda et al., 2016) was 0.43 for Ao which was relatively higher than this study, but Sa showed exactly the same value of 0.26 with this study.

The wood densities (ρ) were 0.557 ± 0.029 g cm^{-3} in Ao, and 0.471 ± 0.039 g cm^{-3} in Sa, respectively. Some other studies reported a relatively higher ρ for both species: 0.654 g cm^{-3} in Ao and 0.521 g cm^{-3} in Sa (Simpson, 1996), 0.670 g cm^{-3} in Ao and 0.559 g cm^{-3} in Sa (Kauffman and Donato, 2012), and 0.63 g cm^{-3} in Ao and 0.50 g cm^{-3} in Sa (Howard et al., 2014), respectively. The results confirmed that ρ of mangrove species were significantly different depending on species and regions (see Appendix 3). However, the ρ values reported by Thant et al. (2012) who studied in Ayeyarwady delta were nearly the same (0.515 g cm^{-3} in Ao and 0.474 g cm^{-3} in Sa) with this study because the study site Yangon region and Ayeyarwady delta were very close and similar tidal conditions. The test results indicated that wood density of Ao was significantly different from the current study but in contrast wood density of Sa was not significantly different (Appendix 3). It pointed out that wood density may be different even at adjacent regions, and collecting site-specific ρ data would be preferable for accurate biomass estimation.

Table 1. Mean stem diameter (*DBH*), mean tree height (*H*), basal area, tree density, relative frequency, relative density, relative dominance, importance value (*IV*) and Shannon index (H') for three species of *Avicennia officinalis* (Ao), *Sonneratia apetala* (Sa) and *S. caseolaris* (Sc).

Species	Mean *DBH* (cm) (min-max)	Mean *H* (m) (min-max)	Basal Area (m^2 ha^{-1}) (Mean ± SD)	Tree Density (ha^{-1}) (Mean ± SD)	Composition parameters				H'
					Relative Frequency	Relative Density	Relative Dominance	*IV*	
Ao	7.11 (5-13.5)	5.57 (4-8.7)	8.69 ± 3.88	2,052 ± 783	58.97	71.08	56.87	186.92	0.243
Sa	9.02 (5-20.9)	7.7 (4-14.2)	9.88 ± 9.23	1,325 ± 917	30.77	23.95	33.75	88.47	0.342
Sc	10.64 (5.1-18)	6.02 (4-7.9)	8.24 ± 6.13	825 ± 512	10.26	4.97	9.38	24.61	0.149
Total					100.00	100.00	100.00	300.00	0.734

Table 2. Summary of characteristics of samples for constructing allometric equations, including range of stem diameter (*DBH*), tree height (*H*), dry/fresh weight ratios of stem, branch and leaves, and wood density (ρ) of dominant species of *Avicennia officinalis* (Ao) and *Sonneratia apetala* (Sa).

Species	n	*DBH* range (cm)	*H* range (m)	dry/fresh weight ratios			ρ (g cm^{-3}) (Mean ± SD)
				Stem (Mean ± SD)	Branch (Mean ± SD)	Leaf (Mean ± SD)	
Ao	15	5−13	5.6−8.2	0.483 ± 0.023	0.474 ± 0.031	0.358 ± 0.061	0.557 ± 0.029
Sa	15	5.1−20	4.6−13.6	0.433 ± 0.043	0.429 ± 0.018	0.257 ± 0.072	0.471 ± 0.039

Allometric equations for Ao, Sa and mixed species

We established several allometric models using biomass components as dependent variables and tree measurable parameters as independent variables. In this section, we provided only the best-fit allometric models for each species and mixed species. The other allometric models tested in this study were tabulated in the Appendices 1−2.

The best-fit allometric equations for leaf, branch, stem and total aboveground biomass of Ao were shown in Table 3. The best explanatory variable was $\rho DBHH$ for leaf biomass ($R^2 = 0.780$, RSS = 2.367), $DBHH$ for branch biomass ($R^2 = 0.922$, RSS = 0.784), ρDBH^2H for stem biomass ($R^2 = 0.965$, RSS = 0.185) and DBH^2H for aboveground biomass ($R^2 = 0.967$, RSS = 0.242), respectively (Fig. 2; Table 3).

The best-fit allometric equations for leaf, branch, stem and total aboveground biomass of Sa were shown in Table 4. The best explanatory variable was ρDBH for leaf biomass ($R^2 = 0.696$, RSS = 8.039), $DBHH$ for branch biomass ($R^2 = 0.925$, RSS = 1.283), DBH^2H for stem biomass ($R^2 = 0.97$, RSS = 0.585) and DBH^2H for aboveground biomass ($R^2 = 0.986$, RSS = 0.254) (Fig. 3; Table 4).

For mixed species, ρDBH^2H was the best independent variable with the highest R^2 value of 0.950 and the smallest errors (RSS = 1.280, MSE = 0.0457) to estimate the total aboveground biomass (Fig. 4; Table 5).

Model comparison with other studies

Comparisons of allometric equations for *A. officinalis,*

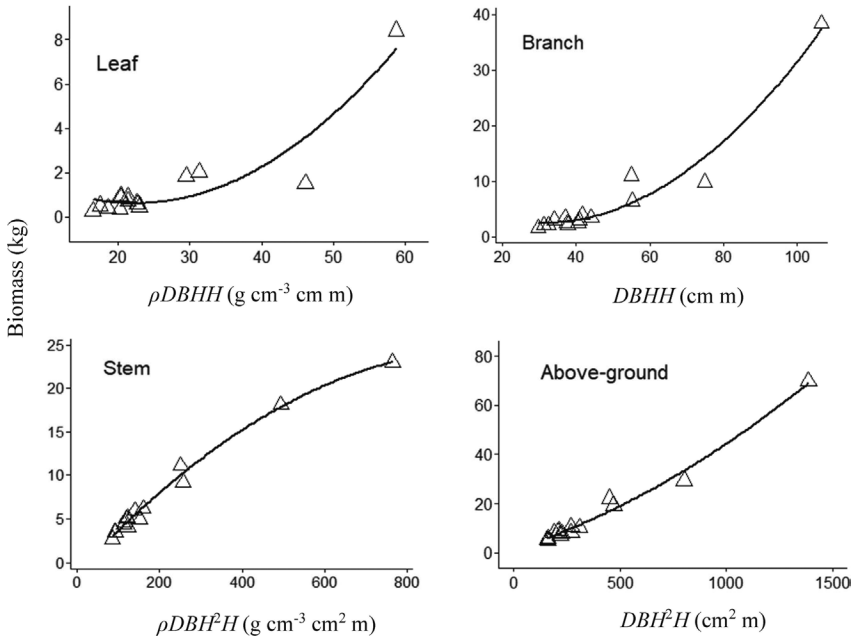


Fig. 2. Relationship between stem diameter DBH (cm), height H (m), wood density ρ (g cm^{-3}) and biomass (kg) of *Avicennia officinalis* (Ao). The curves are based on results of regression analysis using the power function (Table 3).

Table 3. Best fit allometric equations for each biomass component including leaf, branch, stem and aboveground biomass (AGB) of *Avicennia officinalis* (Ao) where DBH, H and ρ mean stem diameter (cm), tree height (m) and wood density (g cm^{-3}), respectively. For each model, coefficient values (a and b), coefficient of determinations (R^2), standard error (SE), residual sum of squares (RSS) and mean squared error (MSE) are shown.

Dependent Variables (y)	Independent Variables (x)	n	a (± SE)	b (± SE)	R^2	SE	RSS	MSE
Leaf (kg)	$\rho DBHH$ (g cm^{-3} cm m)	15	0.0802×10^{-2} ($\pm 0.0826 \times 10^{-2}$)	2.180 (± 0.321)	0.780*	0.427	2.367	0.182
Branch (kg)	$DBHH$ (cm m)	15	0.0574×10^{-2} ($\pm 0.0411 \times 10^{-2}$)	2.340 (± 0.189)	0.922*	0.246	0.784	0.0603
Stem (kg)	ρDBH^2H (g cm^{-3} cm^2 m)	15	0.0489 (± 0.0126)	0.948 (± 0.0504)	0.965*	0.119	0.185	0.0142
AGB (kg)	DBH^2H (cm^2 m)	15	0.0181 ($\pm 0.0600 \times 10^{-1}$)	1.131 (± 0.0583)	0.967*	0.135	0.242	0.0186

* Significant at $p < 0.05$.

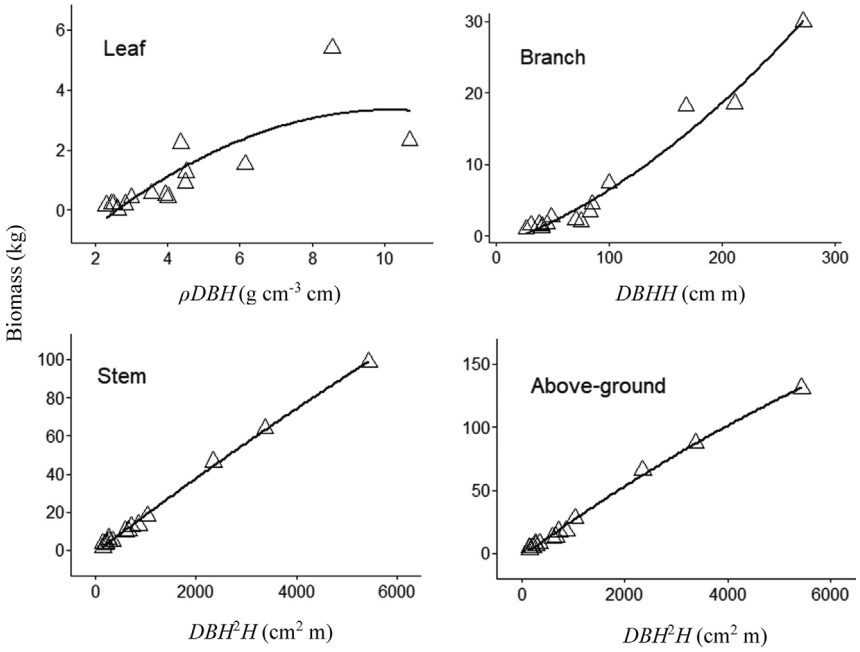


Fig. 3. Relationship between stem diameter *DBH* (cm), height *H* (m), wood density ρ (g cm^{-3}) and biomass (kg) of *Sonneratia apetala* (Sa). The curves are based on results of regression analysis using the power function (Table 4).

Table 4. Best fit allometric equations for each biomass component including leaf, branch, stem and aboveground biomass (*AGB*) of *Sonneratia apetala* where *DBH*, *H* and ρ mean stem diameter (cm), tree height (m) and wood density (g cm^{-3}), respectively. For each model, coefficient values (*a* and *b*), coefficient of determinations R^2, standard error SE, residual sum of squares RSS and mean squared error MSE are shown.

Dependent Variables (y)	Independent Variables (x)	*n*	*a* (± SE)	*b* (± SE)	R^2	SE	RSS	MSE
Leaf (kg)	ρDBH (g cm^{-3}, cm)	15	0.0165 (± 0.0110)	2.519 (± 0.462)	0.696*	0.786	8.039	0.618
Branch (kg)	*DBHH* (cm, m)	15	0.0561×10^{-1} ($\pm 0.0287 \times 10^{-1}$)	1.507 (± 0.119)	0.925*	0.314	1.283	0.0987
Stem (kg)	DBH^2H (cm^2, m)	15	0.0125 ($\pm 0.0411 \times 10^{-1}$)	1.046 (± 0.0506)	0.970*	0.212	0.585	0.0449
AGB (kg)	DBH^2H (cm^2, m)	15	0.0229 ($\pm 0.0493 \times 10^{-1}$)	1.008 (± 0.0334)	0.986*	0.140	0.254	0.0195

* Significant at $p < 0.05$.

S. apetala with other studies are detailed in Table 6. The generalized models from the previous studies conducted in America, Asia, Southern Chian and even Myanmar were also tested in the current study. The *DBH* ranged from 1.7 to 50.0 cm. The model parameters were ρ, *DBH* and *H* respectively. Though some models did not contain *H* in the model, ρ was applied in every generalized model. However, as being less difference for individuals within a species (Van Vinh et al., 2019), ρ was shown as less importance variable in species-specific model.

This study provided species-specific allometric equations for each component of two dominant species. According to the ANOVA results, the site- and species-specific equations from this study showed no significant difference among the models of species-specific, mixed

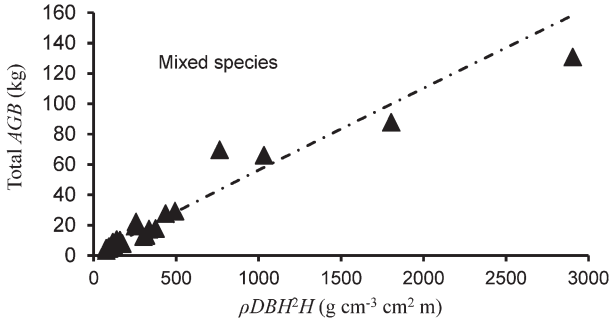


Fig. 4. Relationship between a combined explanatory variable stem diameter *DBH* (cm), height *H* (m), wood density ρ (g cm^{-3}) and biomass (kg) to total aboveground biomass *AGB* for mixed species dataset. The curves are based on results of regression analysis using the power function (Table 5).

Table 5. Allometric equations for aboveground biomass (*AGB*) of mixed species dataset where *DBH*, *H* and *ρ* mean stem diameter (cm), tree height (m) and wood density (g cm^{-3}), respectively. For each model, coefficient values (*a* and *b*), coefficient of determinations (R^2), standard error (SE), residual sum of squares (RSS) and mean squared error (MSE) are shown.

Dependent Variables (y)	Independent Variables (x)	*n*	*a* (± SE)	*b* (± SE)	R^2	SE	RSS	MSE
Mixed (kg)	*DBH* (cm)	30	0.0894 (± 0.0226)	2.450 (± 0.123)	0.934*	0.247	1.707	0.0609
	DBHH (cm m)	30	0.0308 (± 0.0124)	1.498 (± 0.0992)	0.891*	0.317	2.818	0.101
	DBH^2H (cm^2 m)	30	0.0425 (± 0.0136)	0.943 (± 0.0525)	0.920*	0.271	2.057	0.0735
	ρDBH (g cm^{-3} cm)	30	0.483 (± 0.0818)	2.419 (± 0.121)	0.934*	0.246	1.700	0.0607
	ρDBHH (g cm^{-3} cm m)	30	0.0681 (± 0.0178)	1.562 (± 0.0769)	0.936*	0.242	1.642	0.0586
	ρDBH^2H (g cm^{-3} cm^2 m)	30	0.0698 (± 0.0159)	0.969 (± 0.0419)	0.950*	0.214	1.280	0.0457

* Significant at $p < 0.05$.

Table 6. Comparison of allometric equations including mixed species model, *Avicennia officinalis* (Ao) model, and *Sonneratia apetala* (Sa) model in the present study, and the models from other studies, including Komiyama et al. (2005), Thant et al. (2012), and Chave et al. (2005). *AGB* means aboveground biomass (kg), *DBH* means stem diameter at breast height (cm), *H* means tree height (m), n means number of sample trees, and *ρ* means wood density (g cm^{-3}) (0.557 for Ao and 0.471 for Sa). The models were applied for different datasets including mixed species dataset, Ao dataset and Sa dataset.

Data origin	Species	n	*DBH* range (cm)	Models	R^2	Mean estimated *AGB*	SE	Mean difference from observed *AGB*	Sig.*	95% Confidence Level		Source
										Lower	**Upper**	
For mixed species dataset												
Asia	Mixed	104	5−48.9	$AGB=0.251\rho DBH^{2.46}$	0.98	30.45	7.87	−9.11	0.280	14.36	46.54	Komiyama et al. (2005)
Ayeyarwady, Myanmar	Mixed	9	1.7−12.1	$AGB=0.22\rho(DBH^2H)^{0.82}$	0.99	22.93	5.10	−1.59	0.850	12.50	33.35	Thant et al. (2012)
Americas	Mixed	84	5−50	$AGB=0.168\ \rho DBH^{2.47}$	0.99	20.89	5.42	0.45	0.957	9.80	31.98	Chave1 et al. (2005)
Americas	Mixed	84	−42	$AGB=0.0509\ \rho DBH^2H$	−	19.24	5.54	2.10	0.803	7.91	30.58	Chave2 et al. (2005)
Letkhokkon, Myanmar	Mixed	30	5−20	$AGB=0.0698(\rho DBH^2H)^{0.969}$	0.95	21.51	5.94	−0.17		9.35	33.66	**This study**
For Ao dataset												
Letkhokkon, Myanmar	Mixed	30	5−20	$AGB=0.0698(\rho DBH^2H)^{0.969}$	0.95	12.04	2.71	3.08	0.566	6.22	17.86	**This study**
Letkhokkon, Myanmar	Ao (Natural Forest)	15	5−13	$AGB=0.0181(DBH^2H)^{1.131}$	0.97	14.97	4.07	0.15		6.25	23.69	**This study**
For Sa dataset												
Southern China	Sa (Plantation)	12	−	$AGB=0.28(DBH^2H)^{0.693}$	0.99	31.52	7.49	−3.95	0.771	15.46	47.58	Ren et al. (2010)
Letkhokkon, Myanmar	Mixed	30	5−20	$AGB=0.0698(\rho DBH^2H)^{0.969}$	0.95	30.97	11.23	−3.41	0.802	6.88	55.07	**This study**
Letkhokkon, Myanmar	Sa (Natural Forest)	15	5.1−20	$AGB=0.0229(DBH^2H)^{1.008}$	0.99	27.08	9.51	0.48		6.69	47.47	**This study**

species equations reported by the previous studies at 95 % confidence level (Table 6). General model provided by Komiyama et al. (2005) was the highest comparative mean difference from the observed *AGB* among others. In contrast, the model with *ρDBH* variable by Chave1 et al. (2005) expressed the lowest mean difference except the current model. Additionally, the lower/upper bounds of between Chave1 et al. (2005) and current models were

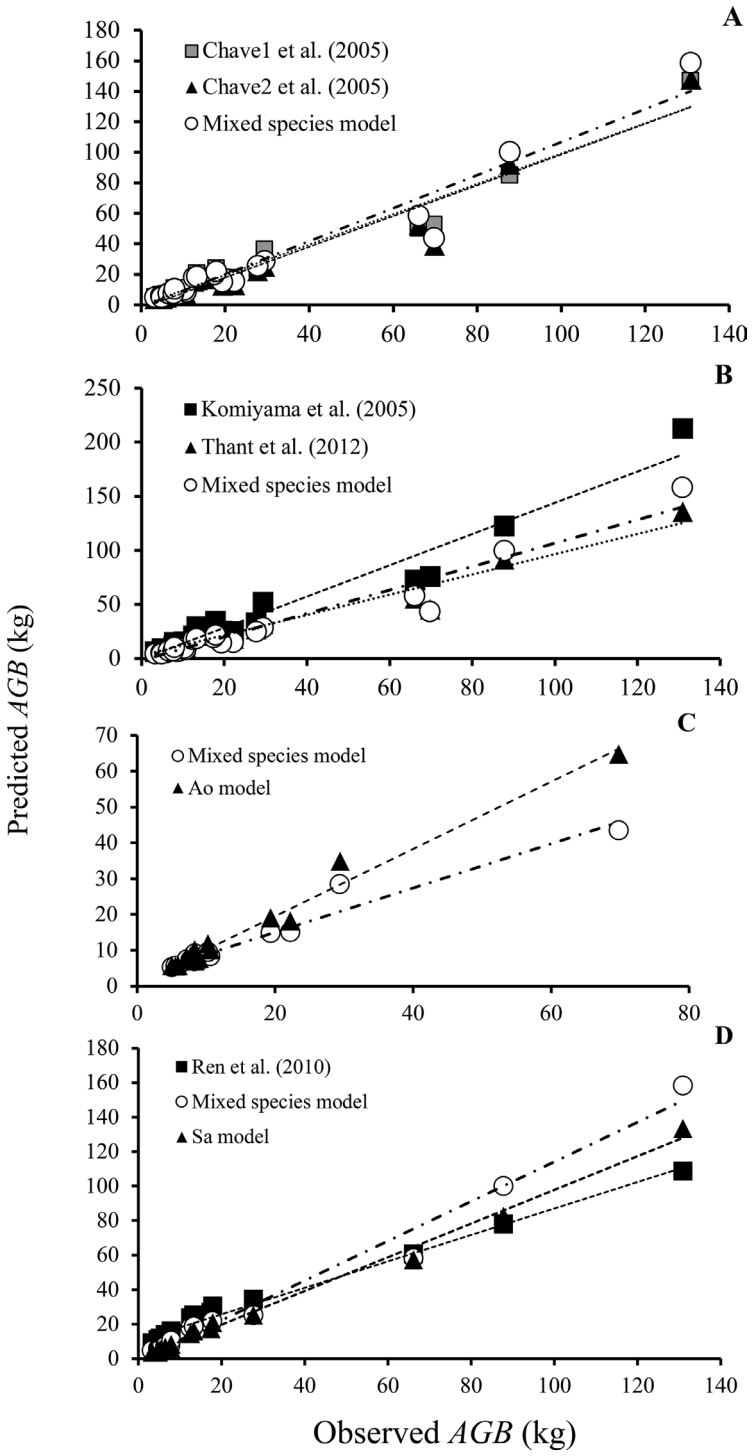


Fig. 5. Comparisons of total aboveground biomass among (A) and (B) mixed species models and other studies, including Chave et al. (2005), Komiyama et al. (2005), and Thant et al. (2012) with mixed species dataset, (C) *Avicennia officianlis* (Ao) model and mixed species model with Ao dataset, and (D) *Sonneratia apetala* (Sa) model, mixed species model and a model from Ren et al. (2010) with Sa dataset.

nearly identical.

However, for site-specific mixed species equation, it was found that the mean aboveground biomass of the current study was largely lower than that estimated by the model using Komiyama et al. (2005). Although Komiyama et al. (2005) developed the model for the mangrove in Southeast Asia, it seemed to overestimate the actual biomass in this study (Fig. 5 B). This finding supported the idea that site-

specific allometric models are crucial to estimate the biomass accurately (Chan and Takeda, 2016; Daba and Soromessa, 2019; Nyamukuru et al., 2023). Also, the estimated biomass by the model developed by Thant et al. (2012) was a bit higher than that by the model of mixed species in this study, despite the research being conducted in the same delta mangrove. Thant et al. (2012) used sample trees including less than 5 cm diameter to develop the allometric model whereas the *DBH* of sample trees in this study was at least 5 cm. It agreed the result by Chan et al. (2013) study that various diameter size classes affect the modelling of biomass estimation. On the other hand, both generalized equations by Chave et al. (2005) who conducted his study in America provided a relatively difference value than this study (Fig. 5 A). One of the general models by Chave et al. (2005) with ρ and *DBH* variables showed a more accurate estimation than the model with ρDBH^2H parameters. This finding points out that accuracy of mangrove allometric model much depends on model parameters, regions, climate, tidal range and sediment characteristics (Phan et al., 2019) and consequently site-specific models are more suitable to be accurate estimation.

Regarding the estimator variables, Komiyama et al. (2005) suggested that the wood density (ρ) should be considered for common allometric model and three models incorporated ρ were into their models (Komiyama et al. 2005, Chave et al. 2005, Thant et al. 2012). Similarly, ρ was significantly important to calculate aboveground biomass in this study (Table 5) and ρDBH^2H was the most significant variable to build the site-specific model for mixed species.

For Ao trees, the mixed species equation underestimated the aboveground biomass and showed lower estimates than the species-specific one (Fig. 5C) because of inter specific differences of canopy form, tree height and wood density. DBH^2H was the most predicted variable for calculating the aboveground biomass of Ao (Appendix 1). The mean biomass difference from the mixed equation was slightly higher than the Ao model. The lower bound of mixed model were nearly the same as the lower bound of Ao model whereas the upper bound of mixed model fell within the upper bound of Ao model. However, those two models were not significantly different at 5 % significance level.

For Sa trees, we made comparisons among an existing equation (Ren et al. 2010), mixed species and species-specific equations (Fig. 5D). The equation of Ren et al. (2010) tended to overestimate the aboveground biomass at smaller tree sizes and tended to underestimate the aboveground biomass at larger tree sizes. While their data were collected from Sa plantation, our data was obtained from natural mangrove forests. This indicates that tree architecture can be changed depending on many environmental variables such as salinity, nutrient availability and inundation periods (Feller et al., 2003; Naidoo, 2006). As Feller et al. (2003) also discussed the complexity of mangrove ecosystem depending on nutrient conditions, different regions reflect different growth patterns. The mixed species equation slightly overestimated the aboveground biomass than the species-specific Sa model (Fig. 5D). As a result of ANOVA, the mean difference from the estimated *AGB* of mixed and Sa equations showed -3.41 kg and 0.48 kg respectively. While the lower bound of mixed model was close to the lower bound of Sa model, upper bound of mixed model was over the upper bound of the Sa model. The DBH^2H was the most significant variable for calculating the aboveground biomass of Sa species. Regarding to Sa trees, the equations including wood density as a part of explanatory variables showed lower R^2 values than the equation having DBH^2H as an explanatory variable (Appendix 2), and DBH^2H was selected as the best explanatory variable to build species-specific model. This suggested that the variation of wood density among individual trees within a species did not significantly explain the variations of aboveground biomass among the individual trees within a species. Though wood density did not significantly differ within a species, it may vary between different parts such as between trunk and branch.

When we tested the generalized and species-specific models of the previous studies to estimate biomass from the current study, some models overestimated and others underestimated the biomass. Generalized models developed by Komiyama et al. (2005) and Thant et al. (2012) exhibited a tendency to overestimate biomass at the site-specific level, while the models by Chave et al. (2005) underestimated it. Also, the mixed species model underestimated biomass at the Ao species-specific level. Additionally, both the mixed species model and the model by Ren et al. (2010) overestimated biomass at the Sa species-specific level. Therefore, our findings suggest that site- and species-specific models are greatly important to estimate biomass considering the accuracy, and also more preferable. This study also proved that wood density which may also reflect the different environmental conditions as well as differences in age and structure species of plantation and natural mangrove, are considerable factors when we developed the allometric models to estimate the biomass.

Biomass and carbon amount of the study site

The estimated biomass in each organ of aboveground parts using the best-fit allometric models for each species

Table 7. Stand biomass and carbon stocks in each component for two dominant species of *Avicennia officinalis* (Ao) and *Sonneratia apetala* (Sa) in Letkhokkon. The values in parentheses mean standard deviations.

Species	Leaf (Mg ha^{-1})	Branch (Mg ha^{-1})	Stem (Mg ha^{-1})	Aboveground parts (Mg ha^{-1})
		Biomass		
Ao	2.2 (± 1.27)	8.91 (± 5.33)	13.39 (± 6.53)	25.55 (± 13.34)
Sa	1.15 (± 1.22)	6.31 (± 7.95)	20.77 (± 26.56)	27.86 (± 34.7)
Total	2.08 (± 1.27)	9.05 (± 6.13)	17.98 (± 16.6)	29.74 (± 22.18)
		Carbon		
Ao	1.1 (± 0.64)	4.46 (± 2.67)	6.7 (± 3.26)	12.77 (± 6.67)
Sa	0.58 (± 0.61)	3.15 (± 3.98)	10.38 (± 13.28)	13.93 (± 17.35)
Total	1.04 (± 0.63)	4.53 (± 3.06)	8.99 (± 8.3)	14.87 (± 11.09)

Note: Data show the average and standard deviation of two dominant species.

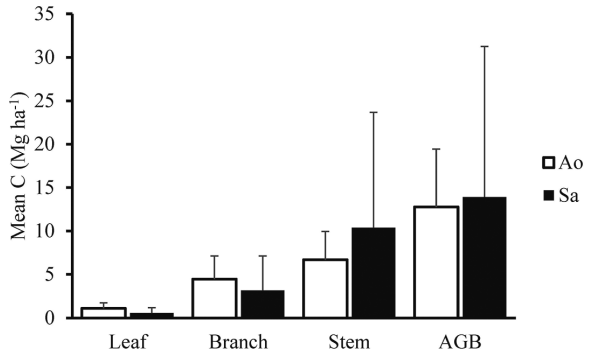


Fig. 6. Average carbon stock (Mg ha^{-1}) of biomass components (leaves, branches, stem, and aboveground biomass *AGB*) for two mangrove species including *Avicennia officinalis* (Ao) and *Sonnenratia apetala* (Sa). Error bar shows standard deviation.

(Tables 3−4 for Ao and Sa, respectively) are listed in Table 7. Ao stand (26 Mg ha^{-1}) had relatively less biomass than Sa stand (28 Mg ha^{-1}). In terms of carbon, Ao stand showed 13 Mg ha^{-1} and Sa stand was 14 Mg ha^{-1} (Fig 6). The total aboveground biomass varies, according to previous studies, with stages of forest development (pioneer, young, mature, and senescent) and also depends on the structural characteristics at each site (Fromard et al., 1998), environmental parameters and climatic factors (Van Vinh et al., 2019). In addition, wood density, tree form and diameter-height relationships between sites can affect the estimation of mangrove biomass (Kauffman and Donato, 2012). Though we considered the some above-mentioned factors such as wood density, *DBH* and *H* variables during model building, other factors such as rainfall patterns, climatic conditions, tidal range and sediment characteristics were not considered when we estimated the aboveground biomass at the stand level in this study.

CONCLUSION

The establishment of species-specific allometric equations, considering parameters such as Diameter at Breast Height (*DBH*), tree height (*H*), and wood density (ρ), provided a tailored approach for biomass estimation, surpassing the limitations of generalized models. The study also highlights the importance of ρ in building site-specific allometric model, emphasizing its influence on accurate biomass calculations.

Comparisons with other studies underscore the significance of site- and species-specific models over general or mixed-species equations, as the former better capture the variability in biomass across different mangrove species. The wood density and plant density as considerable variables for site- and specific-specific equations are crucial, further emphasizing the need for tailored approaches in mangrove biomass estimation.

The biomass and carbon estimations for *A. officinalis* and *S. apetala* in the Letkhokkon area contribute valuable data for understanding the carbon sequestration potential of mangrove ecosystems. Using the models from this study, sequestration rate at species-specific level can be compared at different regions and this valuable biomass data is also supported for the forest management of specific regions. As the differences in structure and influence of environmental factors among species and regions, site- and specific-specific models are better than the generalized ones. Despite environmental constraints at the study site, analyzing the relationships among measurable variables such *DBH*, *H*,

and wood density is essential for model development and comparison, as it provides valuable insights into the site's growth dynamics. The model results also could be applied in the region of Myanmar with the same edaphic conditions where Ayeyarwady delta and Gulf of Mottama. The differences observed in biomass and carbon amounts between the two species suggested the importance of species-specific assessments in understanding the ecological contributions of each mangrove species.

This research not only fills a critical gap in the available biomass data for Myanmar but also provides a basic information to evaluate carbon sequestration potentials that are vital for the management and conservation of mangrove ecosystems in the region. The developed allometric models and biomass estimations contribute to a better understanding of the role of mangroves in global carbon budgets and ecosystem services and attributing to GHG accounting, further facilitating informed decision-making for sustainable coastal management.

Acknowledgements

Funding for this research activity was mainly supported by a charity NGO, Prospect Burma (London, United Kingdom). We sincerely thank Sayar U Win Maung (Project Director - WIF) and staff for their warm support during field activities. We are grateful to the Forest Department (FD) and Letkhokkon CF members, which gave us permission to conduct research in the study area, and besides, the Department of Agriculture - Kungyangon for climatic and rainfall data of 10 years. We kindly show our gratitude to Forest Research Institute (FRI) Yezin, Nay Pyi Taw for oven drying and calculating the wood densities of the mangrove species.

REFERENCES

Bunting P, Rosenqvist A, Lucas RM, Rebelo L-M, Hilarides L, Thomas N, Hardy A, Itoh T, Shimada M, Finlayson CM. 2018. The global mangrove watch—a new 2010 global baseline of mangrove extent. *Remote Sens (Basel)* 10, 1669.

Chan N, Takeda S. 2016. The transition away from swidden agriculture and trends in biomass accumulation in fallow forests: case studies in the Southern Chin Hills of Myanmar. *Mt Res Dev* 36, 320−331.

Chan N, Takeda S, Suzuki R, Yamamoto S. 2013. Establishment of allometric models and estimation of biomass recovery of swidden cultivation fallows in mixed deciduous forests of the Bago Mountains, Myanmar. *For Ecol Manage* 304, 427−436.

Chanda A, Akhand A, Manna S, Das S, Mukhopadhyay A, Das I, Hazra S, Choudhury SB, Rao KH, Dadhwal VK. 2016. Mangrove associates versus true mangroves: a comparative analysis of leaf litter decomposition in Sundarban. *Wetl Ecol Manag* 24, 293−315.

Chave J, Andalo C, Brown S, Cairns MA, Chambers JQ, Eamus D, Fölster H, Fromard F, Higuchi N, Kira T, Lescure JP, Nelson BW, Ogawa H, Puig H, Riéra B, Yamakura T. 2005. Tree allometry and improved estimation of carbon stocks and balance in tropical forests. *Oecologia* 145, 87−99.

Cintron G, Novelli YC. 1984. Methods for studying mangrove structure. In *The mangrove ecosystem: research methods* (ed. Saenger SC, and Snedaker JG), 91−113. UNESCO Monographs in Oceanographic Methodology 8.

Daba DE, Soromessa T. 2019. The accuracy of species-specific allometric equations for estimating aboveground biomass in tropical moist montane forests: case study of *Albizia grandibracteata* and *Trichilia dregeana*. *Carbon Balance Manag* 14, 1−13.

Feller IC, Whigham DF, McKee KL, Lovelock CE. 2003. Nitrogen limitation of growth and nutrient dynamics in a disturbed mangrove forest, Indian River Lagoon, Florida. *Oecologia* 134, 405−414.

Fromard F, Puig H, Mougin E, Marty G, Betoulle JL, Cadamuro L. 1998. Structure, above-ground biomass and dynamics of mangrove ecosystems: new data from French Guiana. *Oecologia* 115, 39−53.

Giesen W, Wulffraat S, Zieren M, Scholten L. 2007. *Mangrove guidebook for Southeast Asia*. Food and Agriculture Organization of the United Nations, Regional Office for Asia and the Pacific, Bangkok, 2006.

Howard J, Hoyt S, Isensee K, Telszewski M, Pidgeon E (Eds.) 2014. *Coastal blue carbon: methods for assessing carbon stocks and emissions factors in mangroves, tidal salt marshes, and seagrasses*. Conservation International, Intergovernmental Oceanographic Commission of UNESCO, International Union for Conservation of Nature. Arlington, Virginia, USA

Huy B, Kralicek K, Poudel KP, Phuong VT, Van Khoa P, Hung ND, Temesgen H. 2016. Allometric equations for estimating tree aboveground biomass in evergreen broadleaf forests of Viet Nam. *For Ecol Manage* 382, 193−205.

Kauffman JB, Donato DC, 2012. *Protocols for the measurement, monitoring and reporting of structure, biomass and carbon stocks in mangrove forests*. Working Paper 86. CIFOR, Bogor, Indonesia.

Khin JJ, Soe AK. 2019. Assessment of Brackish Water Quality from Letkhokkon Area in Yangon Region, Myanmar. *Journal of The Myanmar Academy of Arts and Science* 17, 427.

Kirue B, Kairo JG, Karachi M. 2006. Allometric equations for estimating above ground biomass of *Rhizophora mucronata* Lamk.(Rhizophoraceae) mangroves at Gaxi Bay, Kenya. *Western Indian Ocean Journal of Marine Science* 5, 27−34.

Komiyama A, Havanond S, Srisawatt W, Mochida Y, Fujimoto K, Ohnishi T, Ishihara S, Miyagi T. 2000. Top/root biomass ratio of a secondary mangrove (*Ceriops tagal* (Perr.) CB Rob.) forest. *For Ecol Manage* 139, 127−134.

Komiyama A, Jintana V, Sangtiean T, Kato S. 2002. A common allometric equation for predicting stem weight of mangroves growing in secondary forests. *Ecol Res* 17, 415−418.

Komiyama A, Ong JE, Poungparn S. 2008. Allometry, biomass, and productivity of mangrove forests: A review. *Aquat Bot* 89, 128−137.

Komiyama A, Poungparn S, Kato S. 2005. Common allometric equations for estimating the tree weight of mangroves. *J Trop Ecol* 21, 471−477.

Kusmana C, Hidayat T, Tiryana T, Rusdiana O. 2018. Allometric models for above-and below-ground biomass of *Sonneratia* spp. Glob *Ecol Conserv* 15, e00417.

Magurran AE. 2003. *Measuring biological diversity.* John Wiley & Sons.

Naidoo G. 2006. Factors contributing to dwarfing in the mangrove *Avicennia marina*. *Ann Bot* 97, 1095−1101.

Nyamukuru A, Whitney C, Tabuti JRS, Esaete J, Low M. 2023. Allometric models for aboveground biomass estimation of small trees and shrubs in African savanna ecosystems. *Trees, Forests and People* 11, 100377.

Phan SM, Nguyen HTT, Nguyen TK, Lovelock C. 2019. Modelling above ground biomass accumulation of mangrove plantations in Vietnam. *For Ecol Manage* 432, 376−386.

Ren H, Chen H, Han W. 2010. Biomass accumulation and carbon storage of four different aged *Sonneratia apetala* plantations in Southern China. *Plant Soil* 327, 279−291.

Salem ME, Mercer DE. 2012. The Economic Value of Mangroves: A Meta-Analysis. *Sustainability*. https://doi.org/10.3390/su4030359

Schindler Z, Seifert T, Sheppard JP, Morhart C. 2023. Allometric models for above-ground biomass, carbon and nutrient content of wild cherry (*Prunus avium* L.) trees in agroforestry systems. *Ann For Sci* 80, 28. https://doi.org/10.1186/s13595−023−01196−6

Selvaraj JJ, Gallego Pérez BE. 2023. Estimating mangrove aboveground biomass in the Colombian Pacific coast: A multisensor and machine learning approach. *Heliyon* 9, e20745. https://doi.org/https://doi.org/10.1016/j.heliyon.2023.e20745

Simpson WT. 1996. *Method to estimate dry-kiln schedules and species grouping. Tropical and temperate hardwoods*. USDA, FPL-RP.

Suzuki E, Tagawa H. 1983. Biomass of a mangrove forest and a sedge marsh on Ishigaki Island, South Japan. *Japanese Journal of Ecology* 33, 231−234.

Tamai S, Nakazuga T, Tabuchi R, Ogino K. 1986. Standing biomass of mangrove forests in southern Thailand. *Journal of the Japanese Forestry Society* 68, 384−388.

Thant YM, Kanzaki M, Ohta S, Than MM. 2012. Carbon sequestration by mangrove plantations and a natural regeneration stand in the Ayeyarwady Delta, Myanmar. *Tropics* 21, 1−10.

Van Vinh T, Marchand C, Linh TVK, Vinh DD, Allenbach M. 2019. Allometric models to estimate above-ground biomass and carbon stocks in *Rhizophora apicul*ata tropical managed mangrove forests (Southern Viet Nam). *For Ecol Manage* 434, 131−141.

Wang L, Jia M, Yin D, Tian J. 2019. A review of remote sensing for mangrove forests: 1956−2018. *Remote Sens Environ* 231, 111223. https://doi.org/https://doi.org/10.1016/j.rse.2019.111223

Appendices

Appendix 1. Allometric equations for each component of *Avicennia officinalis*.

Dependent Variables (y)	Independent Variables (x)	*n*	a (± SE)	b (± SE)	R^2	SE estimate	RSS	MSE
Leaf (kg)	*DBH* (cm)	15	0.0556×10^{-1} (± 0.0485)	2.643 (± 0.455)	0.722*	0.480	2.993	0.230
	DBH H (cm, m)	15	0.0195×10^{-2} ($\pm 0.0249 \times 10^{-2}$)	2.215 (± 0.336)	0.770*	0.436	2.477	0.191
	DBH^2H (cm^2, m)	15	0.0834×10^{-2} ($\pm 0.0913 \times 10^{-2}$)	1.218 (± 0.192)	0.756*	0.449	2.624	0.202
	ρ *DBH* (gcm^{-3}, cm)	15	0.0286 (± 0.0166)	2.576 (± 0.434)	0.730*	0.472	2.901	0.223
	ρ *DBH H* (gcm^{-3}, cm, m)	15	0.0802×10^{-2} ($\pm 0.0826 \times 10^{-2}$)	2.180 (± 0.321)	0.780*	0.427	2.367	0.182
	$\rho\ DBH^2H$ (gcm^{-3}, cm^2, m)	15	0.0175×10^{-1} ($\pm 0.0166 \times 10^{-1}$)	1.214 (± 0.186)	0.766*	0.440	2.520	0.194
Branch (kg)	*DBH* (cm)	15	0.0181 ($\pm 0.0946 \times 10^{-1}$)	2.837 (± 0.272)	0.893*	0.287	1.074	0.0826
	DBH H (cm, m)	15	0.0574×10^{-2} ($\pm 0.0411 \times 10^{-2}$)	2.340 (± 0.189)	0.922*	0.246	0.784	0.0603
	DBH^2H (cm^2, m)	15	0.0253×10^{-1} ($\pm 0.0154 \times 10^{-1}$)	1.296 (± 0.107)	0.919*	0.251	0.817	0.0629
	ρ *DBH* (gcm^{-3}, cm)	15	0.115 (± 0.0463)	2.699 (± 0.301)	0.861*	0.328	1.397	0.107
	ρ *DBH H* (gcm^{-3}, cm, m)	15	0.0293×10^{-1} ($\pm 0.0197 \times 10^{-1}$)	2.259 (± 0.210)	0.899*	0.279	1.010	0.0777
	$\rho\ DBH^2H$ (gcm^{-3}, cm^2, m)	15	0.0595×10^{-1} ($\pm 0.0339 \times 10^{-1}$)	1.277 (± 0.111)	0.911*	0.263	0.898	0.0691
Stem (kg)	*DBH* (cm)	15	0.108 (± 0.0246)	2.121 (± 0.119)	0.961*	0.125	0.204	0.0157
	DBH H (cm, m)	15	0.0961×10^{-1} ($\pm 0.0417 \times 10^{-1}$)	1.707 (± 0.115)	0.945*	0.149	0.288	0.0222
	DBH^2H (cm^2, m)	15	0.0267 ($\pm 0.0803 \times 10^{-1}$)	0.956 (± 0.0527)	0.962*	0.123	0.198	0.0152
	ρ *DBH* (gcm^{-3}, cm)	15	0.416 (± 0.0731)	2.043 (± 0.131)	0.949*	0.143	0.264	0.0203
	ρ *DBH H* (gcm^{-3}, cm, m)	15	0.0299 (± 0.0111)	1.666 (± 0.116)	0.941*	0.154	0.308	0.0237
	$\rho\ DBH^2H$ (gcm^{-3}, cm^2, m)	15	0.0489 (± 0.0126)	0.948 (± 0.0504)	0.965*	0.119	0.185	0.0142
AGB (kg)	*DBH* (cm)	15	0.0982 (± 0.0299)	2.488 (± 0.159)	0.949*	0.168	0.367	0.0282
	DBH H (cm, m)	15	0.0511×10^{-1} ($\pm 0.0217 \times 10^{-1}$)	2.033 (± 0.112)	0.962*	0.145	0.275	0.0211
	DBH^2H (cm^2, m)	15	0.0181 ($\pm 0.0600 \times 10^{-1}$)	1.131 (± 0.0583)	0.967*	0.135	0.242	0.0186
	ρ *DBH* (gcm^{-3}, cm)	15	0.484 (± 0.118)	2.385 (± 0.183)	0.929*	0.199	0.513	0.0395
	ρ *DBH H* (gcm^{-3}, cm, m)	15	0.0203 ($\pm 0.0814 \times 10^{-1}$)	1.975 (± 0.125)	0.950*	0.166	0.360	0.0277
	$\rho\ DBH^2H$ (gcm^{-3}, cm^2, m)	15	0.0373 (± 0.0113)	1.118 (± 0.0592)	0.965*	0.140	0.255	0.0196

* Significant at $p < 0.05$.

Appendix 2. Allometric equations for each component of *Sonneratia apetala*.

Dependent Variables (y)	Independent Variables (x)	*n*	a (± SE)	b (± SE)	R^2	SE estimate	RSS	MSE
Leaf (kg)	*DBH* (cm)	15	0.0169×10^{-1} ($\pm 0.0186 \times 10^{-1}$)	2.696 (± 0.508)	0.684*	0.802	8.353	0.643
	DBH H (cm, m)	15	0.0778×10^{-2} ($\pm 0.0111 \times 10^{-1}$)	1.539 (± 0.333)	0.621*	0.877	10.005	0.770
	DBH^2H (cm^2, m)	15	0.0962×10^{-2} ($\pm 0.0125 \times 10^{-1}$)	0.990 (± 0.201)	0.651*	0.842	9.215	0.709
	ρ *DBH* (gcm^{-3}, cm)	15	0.0165 (± 0.0110)	2.519 (± 0.462)	0.696*	0.786	8.039	0.618
	ρ *DBH H* (gcm^{-3}, cm, m)	15	0.0279×10^{-1} ($\pm 0.0309 \times 10^{-1}$)	1.505 (± 0.312)	0.642*	0.853	9.463	0.728
	ρ DBH^2H (gcm^{-3}, cm^2, m)	15	0.0220×10^{-1} ($\pm 0.0243 \times 10^{-1}$)	0.979 (± 0.193)	0.664*	0.826	8.878	0.683
Branch (kg)	*DBH* (cm)	15	0.0175 ($\pm 0.0935 \times 10^{-1}$)	2.463 (± 0.246)	0.885*	0.388	1.956	0.150
	DBH H (cm, m)	15	0.0561×10^{-1} ($\pm 0.0287 \times 10^{-1}$)	1.507 (± 0.119)	0.925*	0.314	1.283	0.0987
	DBH^2H (cm^2, m)	15	0.0811×10^{-1} ($\pm 0.0407 \times 10^{-1}$)	0.945 (± 0.0776)	0.919*	0.325	1.372	0.106
	ρ *DBH* (gcm^{-3}, cm)	15	0.155 (± 0.0587)	2.233 (± 0.262)	0.848*	0.447	2.592	0.199
	ρ *DBH H* (gcm^{-3}, cm, m)	15	0.0219 ($\pm 0.0954 \times 10^{-1}$)	1.443 (± 0.122)	0.915*	0.335	1.455	0.112
	ρ DBH^2H (gcm^{-3}, cm^2, m)	15	0.0191 ($\pm 0.0860 \times 10^{-1}$)	0.920 (± 0.0786)	0.913*	0.337	1.477	0.114
Stem (kg)	*DBH* (cm)	15	0.0265 ($\pm 0.0797 \times 10^{-1}$)	2.776 (± 0.139)	0.969*	0.219	0.622	0.0479
	DBH H (cm, m)	15	0.0900×10^{-1} ($\pm 0.0383 \times 10^{-1}$)	1.651 (± 0.0990)	0.955*	0.261	0.884	0.0680
	DBH^2H (cm^2, m)	15	0.0125 ($\pm 0.0411 \times 10^{-1}$)	1.046 (± 0.0506)	0.970*	0.212	0.585	0.0449
	ρ *DBH* (gcm^{-3}, cm)	15	0.311 (± 0.0899)	2.511 (± 0.200)	0.924*	0.341	1.512	0.116
	ρ *DBH H* (gcm^{-3}, cm, m)	15	0.0402 (± 0.0152)	1.580 (± 0.107)	0.944*	0.292	1.108	0.0852
	ρ DBH^2H (gcm^{-3}, cm^2, m)	15	0.0325 (± 0.0103)	1.017 (± 0.0553)	0.963*	0.237	0.732	0.0563
AGB (kg)	*DBH* (cm)	15	0.0478 (± 0.0115)	2.666 (± 0.111)	0.978*	0.175	0.400	0.0307
	DBH H (cm, m)	15	0.0164 ($\pm 0.0506 \times 10^{-1}$)	1.593 (± 0.0719)	0.974*	0.189	0.466	0.0358
	DBH^2H (cm^2, m)	15	0.0229 ($\pm 0.0493 \times 10^{-1}$)	1.008 (± 0.0334)	0.986*	0.140	0.254	0.0195
	ρ *DBH* (gcm^{-3}, cm)	15	0.505 (± 0.126)	2.418 (± 0.173)	0.938*	0.295	1.129	0.0868
	ρ *DBH H* (gcm^{-3}, cm, m)	15	0.0689 (± 0.0196)	1.527 (± 0.0799)	0.966*	0.219	0.621	0.0478
	ρ DBH^2H (gcm^{-3}, cm^2, m)	15	0.0569 (± 0.0126)	0.981 (± 0.0386)	0.980*	0.165	0.356	0.0274

* Significant at $p < 0.05$.

Appendix 3. Comparing the differences in wood densities of *Avicennia officinalis* (Ao) and *Sonneratia apetala* (Sa) between this study and other studies using One-Sample T Test.

	Wood density	t	df	Sig. (2-tailed)	Mean Difference
For Ao species					
Simpson (1996)	0.654	− 12.912	14	<.001*	− 0.0971
Kauffman and Donato (2012)	0.670	− 15.040	14	<.001*	− 0.113
Howard et al. (2014)	0.63 ± 0.02 SE	− 9.720	14	<.001*	− 0.0731
Thant et al. (2012)	0.515 ± 0.021 SD	5.574	14	<.001*	0.0419
This study	0.557 ± 0.029 SD				
For Sa species					
Simpson (1996)	0.521	− 4.947	14	<.001*	− 0.0501
Kauffman and Donato (2012)	0.559	− 8.697	14	<.001*	− 0.0881
Howard et al. (2014)	0.50 ± 0.01 SE	− 2.875	14	0.012*	− 0.0291
Thant et al. (2012)	0.474 ± 0.042 SD	− .309	14	0.762	− 0.00313
This study	0.471 ± 0.039 SD				

* Significant at $p < 0.05$